mathematics

MDPI

Article

Dynamic Linkages and Asset Allocation Across China's Industrial Chain in the AI Era

Xuemei Yang [1], Wang Gao [1,*] and Yuanyuan Jiang [2]

[1] School of Finance, Hebei University of Economics and Business, Shijiazhuang 050062, China; yangxm@hueb.edu.cn
[2] Department of Computer Science and Technology, Tsinghua University, Beijing 100084, China; amy_jyy@mail.tsinghua.edu.cn
* Correspondence: gaowang@hueb.edu.cn

Abstract

The economic impact of artificial intelligence extends across all stages, including resources, manufacturing, and consumption and services. Against this background, how linkages among the upstream, midstream, and downstream stages of the industrial chain evolve, and what this evolution implies for asset allocation, are important questions for understanding the interaction between technological change and capital markets. Taking the multifactor model as its theoretical starting point, this study uses DCC-ARMA-GARCH to extract dynamic coefficients that measure each stage's response to AI-related information, employs TVP-VAR to characterize cross-stage linkages, and incorporates linkage information into asset allocation. The results show that responses to AI-related information generally exhibit a linkage pattern in which the upstream stage transmits outward and the midstream stage receives transmissions from the other stages. In contrast, overall return linkages feature the midstream stage as the principal transmitter, whereas transmission roles in the former system vary more across periods. Thus, the financial transmission position of the same industrial stage changes with information content and time. Portfolios constructed from AI-related linkage information produce more balanced cross-stage holdings and higher cumulative returns than covariance-based benchmark portfolios, alongside higher volatility and larger drawdowns. By translating each stage's dynamic response to AI changes into information about industrial-chain relationships, this study reveals distinctive connections between the industrial chain and AI and offers a new perspective on industrial-chain linkages and their asset allocation implications in the AI era.

Keywords: AI; industrial-chain linkages; DCC-ARMA-GARCH; asset allocation

MSC: 62M10; 91G10; 91G45

Academic Editor: Zengjing Chen

Received: 28 September 2026
Revised: 26 October 2026
Accepted: 2 November 2026
Published: 4 November 2026

Copyright: © 2026 by the authors. Licensee MDPI, Basel, Switzerland. This article is an open access article distributed under the terms and conditions of the Creative Commons Attribution (CC BY) license.

1. Introduction

Artificial intelligence is expanding from individual technological applications into an important force driving industrial-chain restructuring. Its influence encompasses production organization, factor inputs, and value creation, and extends to the division of labor and cooperation across industrial stages. General-purpose technologies connect industries through broad applicability and complementary innovation, while their

economic benefits depend on complementary investment and organizational adjustment [1,2]. The efficiency effects of generative AI in professional tasks and real-world workplaces further underscore these cross-industry impacts and their heterogeneity [3,4]. From the perspective of the macroeconomic division of production, upstream resource industries, midstream manufacturing industries, and downstream consumption and service industries are interdependent. Industrial-chain restructuring in the AI era involves both adjustments within each stage and the reshaping of cross-stage relationships. Understanding this process requires examining the upstream, midstream, and downstream stages as an interconnected whole, with attention to how a shared technological background interacts with stage-specific differences and how the resulting linkage structures and transmission relationships evolve. Changes in cross-stage relationships also raise new questions for asset allocation: how to identify dynamic adjustments in industrial relationships and use the information they contain in allocation decisions. Examining dynamic industrial-chain linkages and their allocation implications therefore provides an important perspective on the evolution of interindustry relationships in the AI era.

Existing studies explain interindustry interdependence and transmission through production networks and information diffusion [5,6], and further explore the use of network information in portfolio construction [7]. Related AI research examines task structures, firm adoption, and innovation activities, providing multiple perspectives on technological impacts [8,9]. These studies establish a basis for understanding industrial-chain relationships in the AI era. A further issue is how the responses of different stages to AI-related information are interconnected, and how these connections differ from overall industrial-chain comovement. The overall market performance of each stage incorporates diverse operating and market information, whereas its dynamic response to AI-related information offers another perspective on cross-stage adjustment under a specific technological background. Distinguishing these two types of relationships helps extend the analysis of individual stages to the overall relationships within the macroeconomic industrial chain. This study therefore asks what linkage structure emerges among the upstream, midstream, and downstream stages in response to AI-related information, how linkage strength and transmission direction evolve, how this structure differs from overall return linkages, and whether such relational information can be translated into cross-stage allocations with different characteristics.

To address these questions, this study examines linkages among the three stages and their asset allocation implications, starting from each stage's dynamic response to AI-related information. Taking the multifactor model as its theoretical starting point, it establishes a separate trivariate DCC-ARMA-GARCH system comprising each stage's returns, AI-related changes, and CSI 300 returns. Dynamic partial regression coefficients conditional on market returns, termed AI Betas, are calculated from time-varying conditional covariance matrices to characterize each stage's conditional response to AI-related changes. The vector comprising the three Beta series is incorporated into a TVP-VAR model. Generalized forecast error variance decomposition is then used to construct a linkage matrix, distinguishing own-stage explanatory shares from cross-stage explanatory shares, to examine linkage strength, net transmission directions, and their time-varying characteristics, with the raw return system serving as a comparison. On this basis, the innovation covariance matrix and pairwise linkage matrix of the AI Beta system are used to generate weights for covariance-based portfolios and minimum connectedness portfolios, respectively, while a covariance-based portfolio from the raw return system is introduced as a benchmark. All sets of weights are applied to the actual returns of the corresponding industrial-chain stages. Allocation structures and performance are compared under common holding constraints and a consistent return accounting convention to

examine how different relational information is reflected in allocation choices and performance differences.

This study makes three main marginal contributions. First, from the perspective of adjustments in macroeconomic industrial-chain relationships in the AI era, it extends industrial-chain linkage research from overall comovement to the joint adjustment of different stages in response to AI-related information. China's comprehensive industrial system, with its complete range of industries and well-developed supporting capacity, provides an important real-world basis for examining interactions across industrial stages. Drawing on this representative research setting, the study places resources, manufacturing, and consumption and services within the overall industrial division of labor and examines how differentiated responses to a shared technological background form cross-stage relationships. It thus provides evidence from China for understanding AI-related linkages and their evolution in a comprehensive industrial system. Second, it converts AI sensitivity information contained in time-varying conditional covariances into cross-stage linkage matrices and networks, connecting each stage's response strength with its transmission position within the industrial chain. This reveals differences in linkages under the same industrial division of labor across information dimensions and time periods, enriching the understanding of linkage strength and node roles. Third, it uses AI-related linkage information to generate cross-stage allocation weights and compares the resulting portfolios with those based on the innovation covariance matrices of AI Betas and raw returns. By examining differences in holding structures and returns and volatility across information bases, it provides evidence for evaluating the allocation value of industrial relationship information in the AI era.

2. Literature Review

2.1. Research on Industrial-Chain Linkages

Research on industrial-chain linkages is grounded in input–output relationships. It emphasizes that production activities are connected through direct and indirect input dependence, allowing localized shocks to propagate through production networks and generate cross-sector comovement. A sector's network position and connection structure are important for understanding shock propagation and aggregate effects [10,11]. Input substitution and factor reallocation further influence propagation strength and nonlinear responses [12], while changes in technological conditions and input choices also induce adjustments in production network structures [13]. Firm-level evidence shows that input specificity affects the cross-firm propagation of disturbances and that production disruptions can spread through supply chains to direct and indirect upstream and downstream firms [14,15]. Related studies also link network concentration, sparsity, and firms' vertical positions to return performance and exposure to productivity risk [16,17]. These findings indicate that industrial-chain linkages have a clear structural basis: their manifestations depend on the degree of interdependence, the configuration of connections, and the adjustment capacity of different stages.

Research on information diffusion further explains how industrial relationships are reflected in market linkages across economic agents. Information transmission between customers and suppliers, gradual information diffusion within industries, and investor specialization are all associated with lead–lag relationships and cross-predictability in returns [6,18,19]. The ability of some industry returns to predict the overall market is also consistent with the gradual incorporation of industry information into market prices [20]. Changes in the attention of analysts who jointly cover customers and suppliers, and institutional investors who hold shares in both, affect the speed of supply-chain information diffusion [21]. Return predictability also exists among technologically related firms, indicating that information links extend beyond traditional industry boundaries [22].

Interindustry linkages are therefore rooted in the division of production and are also shaped by information content, the scope of attention, and the speed of information absorption. The transmission position of a given industrial stage in different information relationships must be examined in its specific context.

Overall, these studies explain interindustry relationships through production dependence, network structures, and information transmission, providing theoretical and empirical evidence for understanding relational adjustments amid technological change. Building on this foundation, further investigation is needed into the reshaping of macroeconomic industrial-chain linkages in the AI era, particularly how the responses of resources, manufacturing, and consumption and services to AI-related information are connected and how the transmission positions of these stages change over time. Overall return comovement incorporates diverse operating and market information, whereas dynamic responses to AI-related changes offer another dimension for observing cross-stage relationships under a shared technological background. Distinguishing these two types of relationships and comparing their linkage strength, transmission directions, and phase-specific changes from an integrated macroeconomic perspective on the upstream, midstream, and downstream stages provide the starting point for this study and help deepen the understanding of industrial-chain evolution in the AI era.

2.2. The Impact of Artificial Intelligence on the Industrial Chain

The impact of artificial intelligence on the industrial chain combines broad applicability with differentiated adjustment. The distribution of machine learning across industries and research and development activities indicates its potential as a general-purpose technology, providing a basis for understanding AI impacts beyond any single industry [23]. At the same time, differences in the ability structures of occupations and industries correspond to different levels of AI exposure, while actual firm adoption is closely associated with size, complementary digital technologies, and organizational characteristics [8,24]. At the organizational level, automation and human augmentation are interdependent. Realizing the value of technology involves task allocation, decision coordination, and business-process adjustment. When tasks are strongly interdependent, the benefits of an individual application are also constrained by organization-wide arrangements [25,26]. These studies extend AI analysis from specific tasks to production organization and complementary inputs, helping explain differentiated adjustments across industrial-chain stages under a shared technological background.

Empirical evidence further reveals the economic effects of AI on production efficiency, labor demand, and innovation. Experiments involving professional writing and studies of customer-service settings show that generative AI can improve the efficiency of specific tasks, with substantial differences in benefits across skill and experience groups [3,4]. Firm recruitment data show that AI adoption is accompanied by changes in job demand and skill requirements, reflecting the relationship between technology adoption and the division of labor [27]. Corporate AI investment is associated with product innovation and growth, while research on Chinese facial-recognition firms further reveals how access to data supports commercial innovation [9,28]. Related discussions also extend to the channels through which AI affects firm valuation via expectations of future cash flows and information processing [29]. At the aggregate level, the accumulation of gains from localized applications depends on the coverage of affected tasks and the size of those gains, which are important conditions for understanding the scale and heterogeneity of AI's economic effects [30].

Overall, these studies reveal the economic effects of AI through technological exposure, firm adoption, productivity, and innovation. However, there remains scope to investigate the information about dynamic relationships that emerge as industrial-chain

stages respond to AI changes. Existing evidence largely addresses how different agents apply AI, what benefits they obtain, and why these benefits vary. In contrast, systematic empirical evidence remains limited on identifying AI-related dynamic responses within the aggregate changes in resources, manufacturing, and consumption and services, and on revealing the relationships among these responses. Differences in response strength across stages and their joint cross-stage adjustment reflect, respectively, agent-specific and relational aspects of AI's effects. The latter are particularly important for understanding changes in the industrial chain as a whole. This study therefore focuses on the industrial-chain linkage information embedded in AI-related dynamic responses, examining association strength, transmission roles, and their evolution over time to provide a complementary perspective on macroeconomic industrial-chain adjustment in the AI era.

2.3. Industrial-Chain Asset Allocation

Asset allocation research examines the trade-off between returns and volatility when different assets are held jointly. Assets' own return characteristics and their interrelationships together underpin portfolio choice. Classical portfolio theory emphasizes that diversification depends on comovement in asset returns, making covariance relationships central to understanding portfolio risk [31]. Research has further shown that time-varying correlations affect diversification opportunities and optimal holdings. Allocation decisions therefore need to consider adjustments in both individual volatility and common variation [32]. Meanwhile, parameter estimation error can erode the theoretical gains from optimized allocation, making it difficult for complex strategies to consistently outperform simple allocation rules out of sample [33]. These studies indicate that cross-asset allocation hinges on identifying economically meaningful comovement and evaluating the practical value of that information in portfolio management. They provide a theoretical basis for examining allocation relationships among resources, manufacturing, and consumption and service assets.

The network perspective further extends asset allocation analysis to the position of assets within the overall structure of relationships. Research on securities networks shows that network centrality is related to optimal holdings and that an asset's relative position can inform diversification, although its allocation value must also be assessed in conjunction with the asset's own return and volatility characteristics [34]. Cross-asset studies further find that incorporating network structure into investment decisions can improve the return–volatility trade-off in the samples examined, while the realization of such gains also depends on investment objectives and implementation conditions [35]. Research on green bond markets directly incorporates interasset linkages into portfolio management, demonstrating the value of linkage-oriented allocation for improving risk-adjusted performance in the relevant sample [7]. Relationships among assets thus provide both a basis for understanding market comovement and important information for arranging holdings and assessing diversification opportunities.

These studies establish a foundation for combining linkage information with asset allocation, but the allocation implications of changing macroeconomic industrial-chain relationships in the AI era require further investigation. Existing evidence focuses largely on overall return linkages and asset network positions. There has been limited systematic examination of how the joint adjustments of resources, manufacturing, and consumption and services in response to AI changes can inform cross-stage allocation. In particular, whether AI-related linkages offer allocation information distinct from overall price comovement, and how that information changes holding distributions, diversification effects, and the return–volatility trade-off, remain open questions. This study therefore examines the value of AI-related industrial-chain linkages for portfolio management, connecting the identification of dynamic relationships among stages with the arrangement of

cross-stage holdings. By approaching industrial-chain asset allocation through differences in information sources, it provides complementary empirical evidence for investment decisions in the AI era.

3. Research Methods and Data

3.1. Research Models

3.1.1. DCC-ARMA-GARCH and Dynamic Beta Extraction

Multifactor models characterize comovement in asset returns through common factors and their loadings [36]. This study incorporates AI-related changes into a factor framework while using market returns to control for common market movements. A general multifactor return model can be expressed as follows:

$$Y_{i,t} = c_i + \beta_i^M M_t + \sum_{k=1}^{K} b_{i,k} F_{k,t} + u_{i,t} \quad (1)$$

Here, $Y_{i,t}$ and M_t denote the returns of industrial-chain stage i and the market in period t, respectively, and β_i^M is the market factor loading; $F_{k,t}$ denotes factor k other than the market factor, K is the number of such factors, $b_{i,k}$ is the corresponding loading, $u_{i,t}$ is the unexplained component of returns, and c_i is the intercept.

Fixed loadings summarize average sensitivity over the sample period, whereas time-varying conditional covariances further capture how exposures adjust with changing states. Drawing on the modeling approach that connects factor exposures with dynamic covariances [37,38], this study allows the loadings on AI-related changes and market returns to vary over time, extending static sensitivity to daily conditional sensitivity.

This study focuses on the AI factor X_t and includes market returns M_t as a control. Allowing the loadings to vary over time, the conditional linear projection of industrial-chain returns $Y_{i,t}$ is:

$$Y_{i,t} = c_{i,t} + \beta_{i,t}^X X_t + \beta_{i,t}^M M_t + u_{i,t} \quad (2)$$

Here, i corresponds to the upstream, midstream, and downstream stages; $\beta_{i,t}^X$ denotes dynamic AI sensitivity after controlling for common market movements; $\beta_{i,t}^M$ denotes market sensitivity while simultaneously controlling for the AI factor; and $c_{i,t}$ is the intercept. Separate trivariate systems are constructed to characterize the dynamic factor exposures of the industrial-chain stages through time-varying conditional covariances. The AI factor follows an ARMA(1,1) mean equation. Innovations extracted from the mean equations are used to estimate subsequent conditional volatility and correlation structures. Each variable's volatility process is then combined with the dynamic correlations among variables to obtain daily conditional covariance matrices, from which the dynamic sensitivities in Equation (2) are calculated. The industrial-chain subscript i is retained below and refers separately to the upstream, midstream, and downstream stages.

Let $\varepsilon_{i,t} = (\varepsilon_{i,Y,t}, \varepsilon_{i,X,t}, \varepsilon_{i,M,t})'$ denote the mean innovations of system i. To account for persistence in volatility, the three marginal processes follow GARCH(1,1) specifications [39]:

$$h_{i,jj,t} = \omega_{i,j} + \alpha_{i,j}\varepsilon_{i,j,t-1}^2 + \gamma_{i,j} h_{i,jj,t-1}, \qquad j \in \{Y, X, M\} \quad (3)$$

Here, $h_{i,jj,t}$ is the conditional variance of variable j. Variance dynamics are jointly determined by the variance intercept, the most recent squared innovation, and the previous period's conditional variance. Industrial-chain responses to AI changes also depend on relationships among variables. A DCC structure is therefore adopted to decompose conditional covariance into volatility magnitudes and correlations [40]:

$$H_{i,t} = \mathrm{Var}(\varepsilon_{i,t} | \mathcal{F}_{t-1}) = D_{i,t} R_{i,t} D_{i,t} \quad (4)$$

$$D_{i,t} = \mathrm{diag}(\sqrt{h_{i,YY,t}}, \sqrt{h_{i,XX,t}}, \sqrt{h_{i,MM,t}}) \tag{5}$$

The information set $\mathcal{F}_{t-1}$ contains previously available information; $D_{i,t}$ characterizes the volatility magnitudes of the three variables, and $R_{i,t}$ captures their time-varying correlations. Dividing the mean innovations by their respective conditional standard deviations yields the standardized innovations used in the correlation recursion:

$$z_{i,t} = {D_{i,t}}^{-1}\varepsilon_{i,t} \tag{6}$$

Under the DCC(1,1) structure, the correlation state is influenced by both recent innovations and the preceding correlation state:

$$Q_{i,t} = (1 - a_i - b_i)\overline{Q}_i + a_i z_{i,t-1}{z_{i,t-1}}' + b_i Q_{i,t-1} \tag{7}$$

$$R_{i,t} = \mathrm{diag}(Q_{i,t})^{-1/2} Q_{i,t} \mathrm{diag}(Q_{i,t})^{-1/2} \tag{8}$$

Here, $\overline{Q}_i$ is the long-run covariance benchmark for the standardized innovations; a_i and b_i represent the impact of new information and the persistence of the correlation structure, respectively. Both parameters are constrained to be nonnegative, and their sum is less than one. Changes in the variables' own volatilities and their interrelationships jointly form the following conditional covariance matrix:

$$H_{i,t} = \begin{bmatrix} h_{i,YY,t} & h_{i,YX,t} & h_{i,YM,t} \\ h_{i,YX,t} & h_{i,XX,t} & h_{i,XM,t} \\ h_{i,YM,t} & h_{i,XM,t} & h_{i,MM,t} \end{bmatrix} \tag{9}$$

From the conditional linear projection in Equation (2), the dynamic Beta is

$$\beta_{i,t}^{X} = \frac{h_{i,YX,t}h_{i,MM,t} - h_{i,YM,t}h_{i,XM,t}}{h_{i,XX,t}h_{i,MM,t} - {h_{i,XM,t}}^2} \tag{10}$$

Equation (10) captures the conditional sensitivity of industrial-chain returns to AI-related changes given historical information. The volatilities and correlations of the upstream, midstream, and downstream stages adjust daily, producing three dynamic AI Beta series.

Model parameters are obtained through numerical optimization of the likelihood function, and time-varying conditional correlation and conditional covariance matrices are constructed accordingly. Dynamic Betas are calculated from the corresponding elements of the conditional covariance matrices to characterize conditional sensitivities after controlling for overall market movements. Numerical checks include the positive definiteness of the conditional covariance matrices at each date, the positivity of the denominators in the Beta calculations, and the finiteness of the resulting values to ensure that the calculations at each date satisfy the corresponding numerical requirements.

3.1.2. TVP-VAR Linkages and Asset Allocation

Dynamic Betas characterize the sensitivity of individual industrial-chain stages to AI changes, but economic relationships within the industrial chain are also reflected in joint adjustments in sensitivities across stages. This study therefore places the three dynamic AI sensitivity series in a single system to examine how these adjustments are transmitted among the upstream, midstream, and downstream stages. The raw return system serves as a benchmark for comparing price linkages with AI sensitivity linkages.

A vector autoregressive (VAR) model uses each variable's own lags and the lags of other variables to describe the system's dynamic relationships. This study adopts a time-varying parameter vector autoregressive (TVP-VAR) framework, allowing regression coefficients and innovation covariances to change over time to capture phase-specific changes in industrial-chain linkage strength and direction. Compared with rolling-

window VAR models, this framework requires no prespecified window length and avoids the additional loss of observations caused by window truncation [41]. The three dynamic Betas form a vector, and their demeaned series enter the model:

$$b_t = (\beta_{1,t}^X, \beta_{2,t}^X, \beta_{3,t}^X)', \qquad v_t = b_t - \overline{b} \tag{11}$$

Based on the Schwarz Bayesian information criterion [42], the lag order of the AI Beta system is set to one. The model is written as

$$v_t = \sum_{\ell=1}^{p} A_{\ell,t} v_{t-\ell} + u_t, \qquad u_t | \mathcal{F}_{t-1} \sim \mathrm{N}(0, \Sigma_t) \tag{12}$$

Here, $A_{\ell,t}$ describes the effects of the preceding states of the stages on their current states, and Σ_t is the time-varying covariance matrix of system innovations. The coefficient matrices at each lag are stacked into the state vector ϑ_t, whose evolution is expressed as

$$\vartheta_t = \vartheta_{t-1} + \eta_t, \qquad \eta_t | \mathcal{F}_{t-1} \sim \mathrm{N}(0, W_t) \tag{13}$$

Here, η_t is the coefficient-state innovation, and W_t is its covariance matrix. The coefficient state follows the random walk in Equation (13). A Bayesian prior is used for initialization, followed by recursive updating through a Kalman filter with forgetting factors, yielding the response matrices for forecast error decomposition:

$$\Psi_{0,t} = I, \qquad \Psi_{h,t} = \sum_{\ell=1}^{min(p,h)} A_{\ell,t} \Psi_{h-\ell,t}, \qquad h \geq 1 \tag{14}$$

This recursive framework draws on forgetting-factor estimation [43], while the generalized forecast error variance decomposition follows a response construction that is invariant to variable ordering [44]. The forgetting factor is set to 0.99 following Koop and Korobilis [43].

The central question in linkage analysis is what proportion of a stage's future variation is associated with innovations in other stages. Following the forecast error variance decomposition approach [45,46], this study uses generalized decomposition to measure contributions from different sources. For a forecast horizon of H, the contribution of variable j to variable i is

$$g_{ij,t}(H) = \frac{\sigma_{jj,t}^{-1} \sum_{h=0}^{H-1} (e_i' \Psi_{h,t} \Sigma_t e_j)^2}{\sum_{h=0}^{H-1} e_i' \Psi_{h,t} \Sigma_t \Psi_{h,t}' e_i} \tag{15}$$

Here, e_i is a selection vector with one in position i, and $\sigma_{jj,t}$ is diagonal element j of Σ_t. Contributions to each recipient are normalized by row so that the shares from all sources sum to one:

$$\tilde{\theta}_{ij,t}(H) = \frac{g_{ij,t}(H)}{\sum_{k=1}^{n} g_{ik,t}(H)}, \qquad \sum_{j=1}^{n} \tilde{\theta}_{ij,t}(H) = 1 \tag{16}$$

Rows of the normalized matrix represent recipients, and columns represent sources. Diagonal entries are own contributions, and off-diagonal entries are cross-stage contributions. The sample averages of the dynamic shares form the static linkage table:

$$\overline{\tilde{\theta}}_{ij}(H) = \frac{1}{T} \sum_{t=1}^{T} \tilde{\theta}_{ij,t}(H) \tag{17}$$

The total connectedness index summarizes the average share of each stage's variation explained by other stages:

$$\mathrm{TCI}_t = \frac{100}{n} \sum_{i=1}^{n} \sum_{j=1, j \neq i}^{n} \tilde{\theta}_{ij,t} \tag{18}$$

Beyond overall strength, this study distinguishes the extent to which an industrial-chain stage receives influences from other stages from the extent to which it transmits

influences to them. The former is obtained by summing off-diagonal shares along rows, and the latter by summing them along columns:

$$\mathrm{FROM}_{i,t} = 100 \sum_{j=1, j\neq i}^{n} \tilde{\theta}_{ij,t} \tag{19}$$

$$\mathrm{TO}_{i,t} = 100 \sum_{j=1, j\neq i}^{n} \tilde{\theta}_{ji,t} \tag{20}$$

$$\mathrm{NET}_{i,t} = \mathrm{TO}_{i,t} - \mathrm{FROM}_{i,t} \tag{21}$$

Positive net transmission indicates that a stage transmits a larger share outward than it receives, whereas a negative value indicates net reception. To identify specific transmission directions within the network, the two directional contributions are compared for each pair of stages:

$$\mathrm{NPDC}_{ij,t} = 100(\tilde{\theta}_{ij,t} - \tilde{\theta}_{ji,t}) \tag{22}$$

Under the row–column convention above, $\mathrm{NPDC}_{ij,t} > 0$ indicates net transmission from j to i; a negative value indicates the reverse direction. Network arrows are determined by these net transmission values. Asset allocation additionally requires a measure of the two-way relationship between each pair of stages. The pairwise connectedness index is defined as

$$\mathrm{PCI}_{ij,t} = 200 \frac{\tilde{\theta}_{ij,t} + \tilde{\theta}_{ji,t}}{\tilde{\theta}_{ii,t} + \tilde{\theta}_{ij,t} + \tilde{\theta}_{ji,t} + \tilde{\theta}_{jj,t}} \tag{23}$$

The pairwise connectedness indices form a symmetric matrix, C_t, translating the strength of joint industrial-chain adjustment into information for allocation. Focusing on the minimum connectedness portfolio (MCoP), this study examines the cross-stage holdings and performance associated with AI sensitivity linkages and uses covariance-based portfolios (MVPs) as comparison benchmarks. The MCoP uses the pairwise linkage matrix of AI Betas; the MVPs use the innovation covariance matrix of the AI Beta system, $\Sigma_{\beta,t}$, and that of the raw return system, $\Sigma_{r,t}$, respectively, to construct weights. All portfolios are evaluated using actual industrial-chain returns, with dynamic Betas supplying allocation information.

Following Broadstock et al. [7], the MCoP and MVPs use inverse-matrix weights. Let S_t denote the covariance matrix used for an MVP, taken from either the AI Beta or the raw return system's innovation covariance; 1 denotes a vector of ones, and $\dagger$ denotes the Moore–Penrose generalized inverse. The initial weights for the two types of portfolios are

$$v_t^{\mathrm{MCoP}} = \frac{{C_t}^{\dagger} 1}{1' {C_t}^{\dagger} 1} \tag{24}$$

$$v_t^{\mathrm{MVP}} = \frac{{S_t}^{\dagger} 1}{1' {S_t}^{\dagger} 1} \tag{25}$$

The MCoP maps the pairwise linkage structure of AI sensitivities into allocation weights, while the MVPs provide a comparison of holdings based on covariance information. The initial weights are restricted to the interval [0,1] and then normalized so that their sum equals one:

$$w_{i,t}^{k} = \frac{\min\{1, \max\{0, v_{i,t}^{k}\}\}}{\sum_{j=1}^{n} \min\{1, \max\{0, v_{j,t}^{k}\}\}}, \qquad \mathrm{k} \in \{\mathrm{MCoP}, \mathrm{MVP}\} \tag{26}$$

For portfolio evaluation, each asset's daily log return is first converted into a simple return: $R_{i,t} = e^{r_{i,t}} - 1$.

Let R_t denote the vector of daily simple returns for the three industrial-chain stages. Applying the previous period's weights to current returns, the portfolio's daily simple return is

$$R_{p,t}^k = w_{t-1}^{k\prime} R_t \tag{27}$$

Cumulative returns are calculated by compounding the portfolio's daily simple returns over successive periods:

$$I_{p,\tau}^k = \prod_{t=1}^{\tau}(1 + R_{p,t}^k) - 1 \tag{28}$$

Allocation performance is further evaluated in terms of returns, volatility, drawdowns, and hedging effectiveness. Let T_p be the number of valid return observations, and let $\overline{R}_p$ and s_p be the sample mean and sample standard deviation of the portfolio's daily simple returns, respectively. Annualized returns are calculated using geometric compounding, and volatility is annualized from the daily standard deviation using 252 trading days:

$$\mathrm{AR}_p = (1 + I_{p,T_p})^{\frac{252}{T_p}} - 1, \qquad \mathrm{AV}_p = \sqrt{252}s_p \tag{29}$$

Under an evaluation convention that sets the risk-free return to zero, the Sharpe ratio is defined as

$$\mathrm{SR}_p = \sqrt{252}\frac{\overline{R}_p}{s_p} \tag{30}$$

The cumulative path is also used to measure the largest decline from a preceding peak:

$$\mathrm{MDD}_p = \min_{0\le\tau\le T}\left[\frac{1 + I_{p,\tau}}{\max_{0\le s\le\tau}(1 + I_{p,s})} - 1\right] \tag{31}$$

Here, the initial value of the cumulative path is zero. Hedging effectiveness compares the variance of portfolio returns with that of holding the reference asset alone, using simple returns:

$$\mathrm{HE}_i = 1 - \frac{\mathrm{Var}(R_{p,t})}{\mathrm{Var}(R_{i,t})} \tag{32}$$

Higher hedging effectiveness indicates a larger variance reduction relative to the reference asset. This study evaluates the allocation implications of AI sensitivity information jointly through linkage structures, portfolio weights, and performance measures.

3.2. Data and Variables

This study uses the CSI Industrial Chain Index Series compiled by China Securities Index Co., Ltd. (Shanghai, China), comprising the CSI Upstream Resources Industry Index (000961.CSI), the CSI Midstream Manufacturing Industry Index (000962.CSI), and the CSI Downstream Consumption and Services Industry Index (000963.CSI). Drawing its sample universe from the constituents of the CSI 800 Index, the series selects securities of larger listed companies in the Shanghai and Shenzhen markets with the corresponding industrial-chain characteristics. The three indices reflect the market performance of upstream resource industries, midstream manufacturing industries, and downstream consumption and service industries, respectively, providing representative index samples for studying dynamic linkages and asset allocation across industrial-chain stages. According to the Methodology for the CSI Industrial Chain Index Series, securities within each of the three industrial categories are ranked in descending order of average daily total market

capitalization over the preceding year to form the corresponding index constituents. Constituent adjustments and index maintenance follow the official rules. Daily closing levels for the three indices are obtained from the Wind database and used to calculate daily log returns as proxies for the return performance of the upstream, midstream, and downstream stages.

Under the official classification, the upstream index includes oil, natural gas, coal, non-ferrous metals, and non-metallic mining and products, while the midstream index includes chemicals, steel, machinery, and communications equipment. The downstream index includes automobiles, consumer services, consumer durables and apparel, food and beverages, healthcare, and telecommunications services. As an illustrative constituent snapshot, the official factsheets for 2026 list Zijin Mining and China Shenhua among the major upstream constituents, Contemporary Amperex Technology and Foxconn Industrial Internet among the major midstream constituents, and Kweichow Moutai and Midea Group among the major downstream constituents.

This study uses the AI-E (Economy) index as the AI-related variable. The index counts newspaper articles containing both artificial-intelligence and economy-related keywords, scales the daily matching count by the total number of newspaper articles that day, and normalizes the 2015–2021 mean to 100, capturing the relative intensity of AI-related economic topics. The data are obtained from https://www.policyuncertainty.com/aieu_daily.html (accessed on 18 September 2026). The AI-E index measures the frequency of newspaper coverage jointly addressing artificial intelligence and economic topics and serves as a proxy for AI-related economic information. Related AI information has been used to study stock market volatility and risk transmission [47,48]. The CSI 300 Index represents the broad market. Its daily closing levels are obtained from the Wind financial terminal and used to calculate daily log returns as the market control variable. The sample comprises 2847 trading days from 6 January 2015 to 18 September 2026. The data were accessed on 18 September 2026, and model estimation was completed on 21 September 2026. All datasets used in the analysis were available at the time of access. All series are aligned on common stock trading dates to maintain temporal consistency across variables.

Table 1 reports descriptive statistics for the series. The mean log returns of the upstream, midstream, and downstream stages are all positive and close to zero, and their volatilities decrease in that order, indicating differences in return fluctuations across industrial stages. All series exhibit left skewness and fat tails. The JB test [49] rejects normality, while the ADF and PP tests [50,51] reject the unit-root hypothesis. The Q(20), Q^2(20), and ARCH-LM(10) tests indicate serial correlation and conditional heteroskedasticity, supporting the modeling of time-varying conditional volatility alongside mean dynamics.

Table 1. Descriptive statistics.

Variable	Mean	Std. Dev.	Skewness	Kurtosis	JB	ADF	PP	Q(20)	Q^2(20)	ARCH-LM(10)
CSI upstream	0.000173	0.017613	−0.597	6.129	1325.246***	−52.235***	−52.257***	35.674**	1239.519***	372.927***
CSI midstream	0.000193	0.017031	−0.603	7.837	2935.866***	−51.468***	−51.575***	36.605**	1684.365***	456.850***
CSI downstream	0.000060	0.014706	−0.611	8.026	3160.993***	−51.019***	−50.997***	67.385***	1922.656***	496.843***
AI-E	0.001674	0.947957	−0.059	8.819	4001.190***	−20.763***	−263.098***	728.423***	1733.963***	618.371***
CSI 300	0.000075	0.013597	−0.758	9.852	5819.232***	−52.046***	−52.031***	81.898***	1401.067***	413.018***

Note: ** and *** indicate rejection of the corresponding null hypothesis at the 5% and 1% levels, respectively.

4. Empirical Results and Analysis

4.1. Dynamic Beta Results

Table 2 reports the key parameters and diagnostics for the three DCC-ARMA-GARCH models. All three models converge successfully, the sums of their DCC parameters are below one, and conditional correlations exhibit strong persistence. The conditional covariance matrices and the denominators in the Beta calculations pass basic numerical checks. For the Q(20), Q^2(20), and ARCH-LM(10) tests of standardized marginal residuals, all p-values for the Y, X, and M margins in the three systems exceed 0.10. There is no significant remaining linear serial correlation, squared serial correlation, or ARCH effect at the selected lags [52,53]. The results indicate a good model fit.

Table 2. Evaluation of DCC-ARMA-GARCH results.

Industrial Stage	Residual Variable	DCC-*a*	DCC-*b*	*a* + *b*	Beta Mean	Beta Std. Dev.	Q(20)	Q^2(20)	ARCH-LM(10)
Upstream	Y	0.0262	0.9643	0.9905	0.000491	0.002374	18.491	15.461	6.852
	X						22.404	2.560	1.034
	M						23.866	8.853	3.844
Midstream	Y	0.0268	0.9594	0.9862	0.000706	0.001347	19.906	10.339	6.231
	X						22.404	2.560	1.034
	M						23.866	8.853	3.844
Downstream	Y	0.0312	0.9611	0.9923	0.000110	0.001326	22.773	13.328	7.304
	X						22.404	2.560	1.034
	M						23.866	8.853	3.844

Note: Y, X, and M denote the corresponding industrial-chain stage, AI, and the CSI 300, respectively. The DCC parameters *a* and *b* govern the impact of the latest standardized innovations and the carryover of the previous correlation state, respectively.

Figure 1 presents the dynamic Betas of the upstream, midstream, and downstream stages. The sample means of all three series are positive, but their signs change during some periods, indicating pronounced time variation in the conditional sensitivity of industrial-chain returns to AI changes. Differences also exist across stages: the midstream stage has a higher average sensitivity, sensitivity fluctuations are more pronounced in the upstream stage, and the downstream stage has a relatively low average sensitivity. Overall, the conditional associations of industrial-chain stages with AI changes adjust over time in both direction and strength, exhibiting distinct stage-level heterogeneity.

4.2. Industrial-Chain Linkage Results

4.2.1. Static Linkage Analysis

Table 3 reports AI sensitivity linkages across the upstream, midstream, and downstream stages, while own-stage explanatory shares remain dominant, indicating the coexistence of stage-specific dynamics and joint adjustment. In terms of overall pairwise strength, upstream–midstream linkages are relatively strong, followed by upstream–downstream linkages, whereas midstream–downstream linkages are relatively weak. However, the differences in strength across the three pairs are limited. This indicates that AI sensitivity linkages span resources, manufacturing, and consumption and services, without being highly concentrated in any single pair of industrial relationships. Overall, industrial-chain relationships in the AI era show a degree of integration while retaining substantial stage-level heterogeneity: sensitivity changes across stages are interconnected and retain their own characteristics.

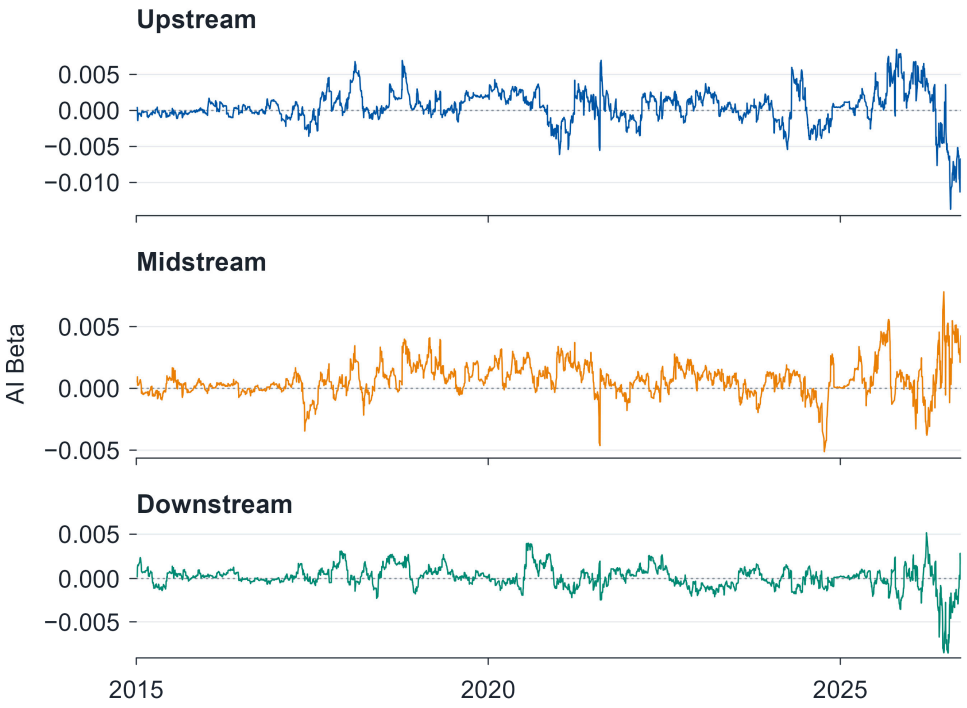


Figure 1. Dynamic Betas of the upstream, midstream, and downstream stages with respect to AI.

This pattern reflects production dependence and technological complementarity. Input relationships connect adjustments in resources and manufacturing, while substitution opportunities and conditions for resource reallocation differentiate intersectoral relationships [5,12]. AI applications also require complementary investment in organization, data, and processes, and the conditions for adaptation and the realization of benefits differ across stages [2,26]. From this perspective, the relatively strong upstream–midstream linkage and the predominance of own-stage information correspond to two dimensions: industrial input dependence and heterogeneity in technological responses. Industrial-chain linkages in the AI era thus reflect joint adjustment while retaining independent variation associated with different production functions.

By comparison, the estimated TCI is 50.08% for raw returns and 26.55% for AI Betas, a difference of 23.53 percentage points. The raw-return system also has the closest relationship between the midstream and downstream stages and more pronounced differences in strength across industrial pairs. AI Betas exhibit weaker cross-stage linkages and a more even distribution of linkage strength, with a more prominent upstream–midstream relationship. This difference reflects the information content of the two types of linkages. Raw returns jointly reflect industrial operations, market expectations, and other information, with manufacturing and consumption and services more closely connected in overall price changes. AI Betas instead focus on each stage's sensitivity to AI-related changes, highlighting the coexistence of joint adjustment and differentiated responses under a technological background. Strong connections in the overall market performance of the industrial chain therefore do not imply equally strong AI sensitivity linkages. AI-related relationships reveal connections within the industrial chain that differ from those captured by aggregate price changes.

Table 3. Static linkage matrices of AI Betas and raw returns for the CSI industrial chain.

Variable/ Indicator	Data	Upstream	Midstream	Downstream	FROM
Upstream	AI Beta	74.65	12.75	12.61	25.35
Midstream	AI Beta	15.75	71.85	12.40	28.15
Downstream	AI Beta	14.52	11.63	73.85	26.15
TO	AI Beta	30.27	24.38	25.00	TCI = 26.55
Upstream	Raw returns	52.98	27.92	19.11	47.02
Midstream	Raw returns	24.64	46.14	29.22	53.86
Downstream	Raw returns	18.03	31.33	50.64	49.36
TO	Raw returns	42.67	59.25	48.32	TCI = 50.08

Note: The two systems comprise dynamic AI Betas and raw log returns, respectively. Rows represent recipients and columns represent sources. FROM and TO denote the shares received from and transmitted to other stages, respectively; TCI is the total connectedness index. All values are percentages.

4.2.2. Network Structure Analysis

Panel A of Figure 2 shows distinct node roles in the AI Beta net transmission network. Net transmission and reception refer to model-based predictive connectedness derived from forecast error variance decomposition. The upstream stage transmits to both the midstream and downstream stages in net terms and is the network's principal transmitter, with net pairwise connectedness of approximately 3.0 and 1.9 percentage points, respectively. The midstream stage receives net transmissions from both the upstream and downstream stages, forming a concentrated reception structure. The downstream stage combines reception and transmission: it receives net transmission from the upstream stage while transmitting to the midstream stage. Although the downstream stage is a net receiver in the overall system, it acts as a net transmitter in its bilateral relationship with the midstream stage, demonstrating that node roles depend on the specific counterpart. Overall, the network features outward transmission from the upstream stage and convergence toward the midstream stage from both the upstream and downstream stages, highlighting distinct stage roles within AI sensitivity linkages.

This directional pattern can be interpreted through the interaction between input connections and technological adaptation. Upstream resources enter multiple production stages, while manufacturing connects input procurement with end-use applications. Input choices and vertical positions under technological change therefore have different valuation implications [13,17]. In this study's network, the upstream stage's outward links reflect cross-stage information contained in adjustments to resource-sector AI sensitivity. The midstream stage's position as a convergence point reflects its simultaneous association with supply-side and demand-side changes, while the downstream stage participates in sensitivity transmission through demand and application relationships.

Industry-level AI exposure varies with the occupational abilities and tasks involved, while existing research documents substantial sectoral differences in AI adoption [8,24]. For the industries represented here, a plausible transmission channel is that AI-related economic information changes expectations about energy and material demand in resource industries, production and equipment upgrading in manufacturing, and product and service applications downstream. Energy and raw materials connect the upstream index to multiple purchasing industries, so adjustments in resource-sector AI sensitivity can contain information relevant to costs and investment across the chain. Evidence on supplier-shock propagation and the asset-pricing role of production networks [14,16] supports interpreting the upstream stage's prominent outward links in terms of these broad input connections.

By comparison, the raw return network in Panel B features the midstream stage as the principal transmitter, with the upstream stage receiving net transmissions from the midstream and downstream stages. The difference between the two networks reflects the information dimension under examination. Returns jointly reflect costs, demand, and earnings expectations, so market changes in manufacturing contain information relevant to upstream and downstream operations. The gradual absorption of customer information and differences in investors' information coverage provide a pricing explanation for return linkages from the midstream and downstream stages toward the upstream stage [6,19]. AI Betas instead focus on adjustments in technology-related sensitivity, and the reach and pricing of technological information can extend beyond established industry relationships [22]. The same industrial stage therefore holds different transmission positions in the overall price network and the AI sensitivity network. These model-based network roles can be interpreted in relation to industrial specialization and the type of information examined.

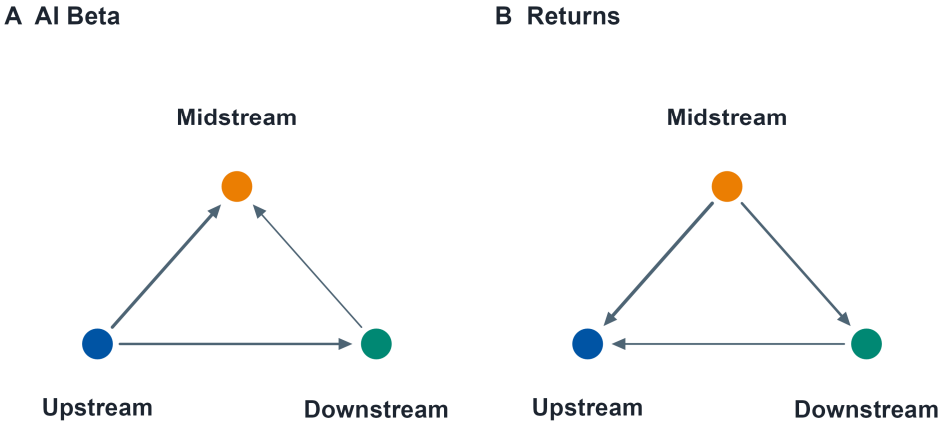


Figure 2. Transmission networks. Note: (**A**) shows AI Betas and (**B**) shows raw returns. Arrows point from net transmitters to net receivers, and line widths represent pairwise net transmission strength.

4.2.3. Dynamic Linkage Analysis

Figure 3 shows that overall industrial-chain AI sensitivity linkages alternate between phases of strengthening and decline, combining persistent adjustment with localized surges. Early in the sample, the TCI of AI Betas gradually decreases from a relatively high level and moves into a lower fluctuation range. Linkages strengthen markedly in the middle of the sample, forming a relatively strong phase around 2022. They subsequently decline overall, with local rebounds alternating with weaker linkages, before rising again near the sample end. This process indicates continual shifts between joint adjustment and differentiated variation in the AI sensitivities of the upstream, midstream, and downstream stages. By comparison, the TCI of raw returns is higher during most periods. The turning points and adjustment magnitudes of the two systems differ, indicating distinct temporal patterns in overall industrial-chain price relationships and AI sensitivity relationships.

This evolution can be interpreted through the alternating effects of shared technological expectations and differentiated industrial adaptation. The benefits of AI depend on complementary inputs and organizational coordination, while adaptation and benefit realization proceed at different speeds across stages [2,26]. Evidence on generative AI's effects on task efficiency and real-world workplaces provides a microeconomic basis for understanding the translation of technological potential into application-specific gains [3,4]. From this theoretical perspective, stronger linkages reflect more concentrated sensitivity adjustments to common information, whereas subsequent declines reflect the renewed prominence of stage-specific differences. The phase changes shown in the figure thus reflect an alternation between common expectations and differentiated responses.

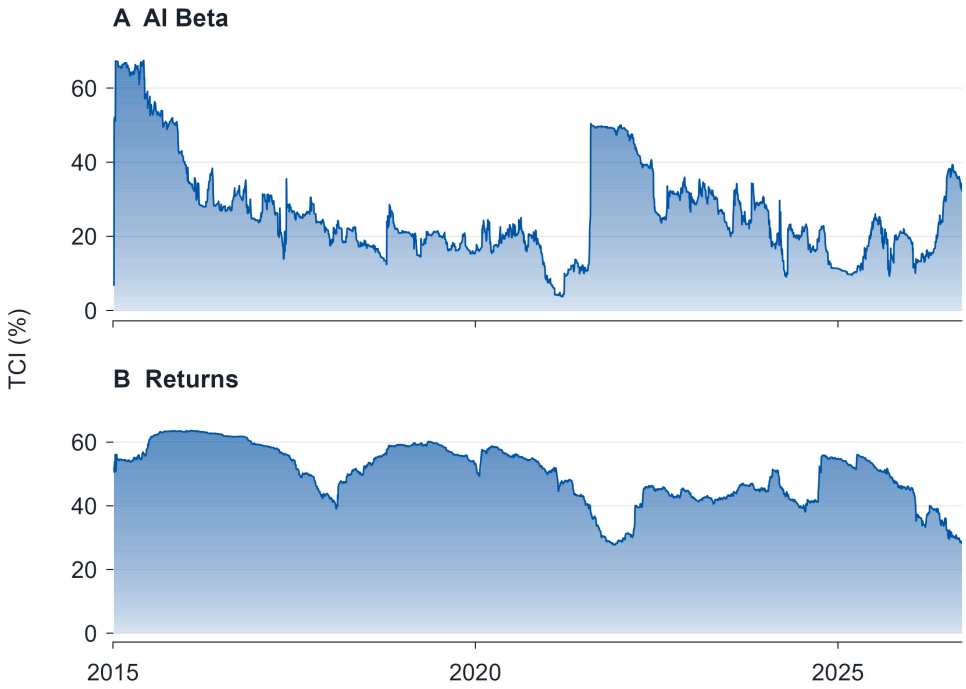


Figure 3. Dynamic TCI.

Figure 4 shows pronounced variation over time in the net transmission roles of industrial-chain stages within AI sensitivity linkages, with all three stages switching between net transmission and net reception. In Panel A, the upstream stage is a relatively strong net transmitter for part of the early sample, while the midstream stage primarily acts as a net receiver; their roles subsequently reverse several times. Around 2022 and for a period thereafter, the upstream and downstream stages more often act as net transmitters, while the midstream stage's net reception is pronounced. Later in the sample, the upstream stage experiences a distinct net-reception phase, with the midstream and downstream stages becoming net transmitters, before the pattern adjusts again near the sample end. The downstream stage also participates in changes in net transmission directions across periods, reflecting continual adjustment in interactions among the three stages. By comparison, the raw return linkages in Panel B display greater persistence in node roles: the midstream stage remains a net transmitter for most of the sample, and the upstream stage primarily acts as a net receiver. The two systems therefore differ: node roles in return linkages are relatively stable, whereas transmission positions in AI sensitivity linkages are more phase-dependent.

Switches in net transmission roles further reflect the joint effects of industrial position and the focus of information pricing. Technological change alters input choices and valuation exposures at different vertical stages, while the speed of information absorption is influenced by the attention of investors connected to those stages [17,21]. Compared with aggregate price changes, AI sensitivity emphasizes the market's relative responses to information about resource inputs, manufacturing adaptation, and end-use applications. Different stages alternate as important information sources, generating phase-specific switches between outward and inward links. AI affects multiple dimensions, including technology applications, expectations, and information processing, providing a theoretical background for the greater phase dependence of its linkage roles relative to those of raw returns [29].

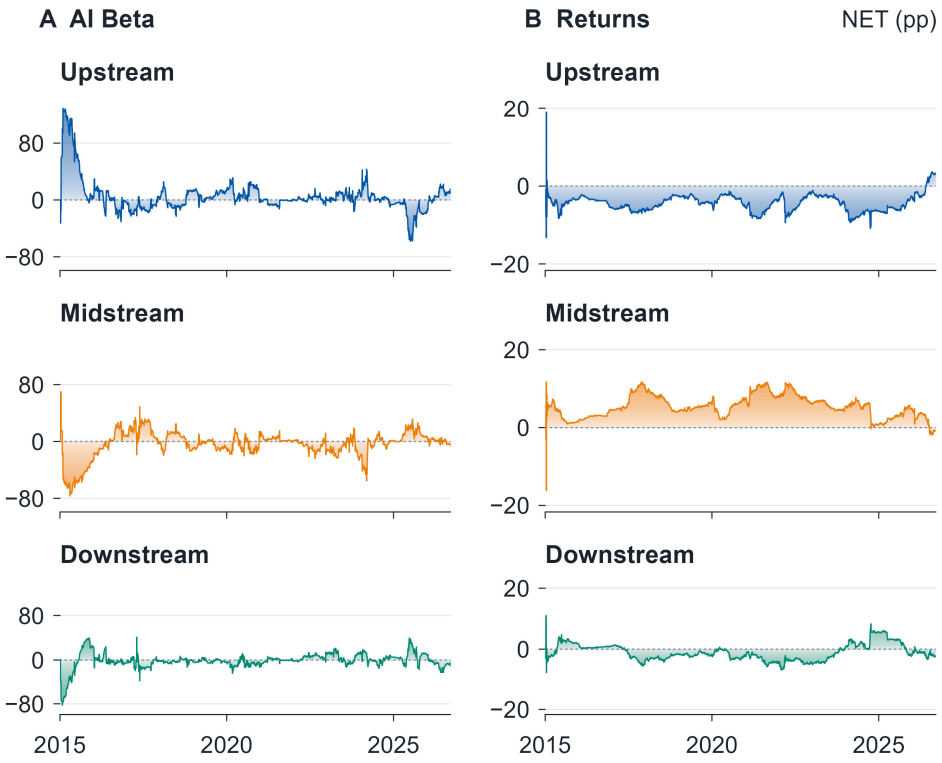


Figure 4. Dynamic NET.

Dynamic adjustments in net transmission roles and pairwise relationships provide additional state information for industrial-chain allocation. Asset allocation must account for both the volatility of individual stages and cross-stage comovement, and changes in correlation structures can influence capital allocation and holding adjustments [32]. This study further maps pairwise AI sensitivity linkages into weights to examine how they differ from allocations guided by the covariances of AI Betas and raw returns.

4.3. Asset Allocation Results

4.3.1. Allocation Structure and Portfolio Performance

Table 4 shows that the MCoP produces relatively balanced average allocations across the upstream, midstream, and downstream stages, with substantial participation by all three. Compared with the two MVPs, the MCoP increases the weights of the upstream and midstream stages and reduces concentration in the downstream stage. Both MVPs allocate more heavily to the downstream stage, with the raw-return-based allocation

being the most concentrated; the AI-Beta-based allocation increases the participation of manufacturing. Pairwise AI sensitivity linkage information thus corresponds to a more balanced industrial-chain allocation, incorporating resources, manufacturing, and consumption and services into portfolio holdings.

The MCoP's holding structure illustrates the role of industrial-chain linkage information in asset allocation. Its weights are determined by each stage's pairwise relationships with the entire system, incorporating joint cross-stage adjustments in AI sensitivities into capital allocation. The MVPs provide covariance-based comparisons. The effects of network relationships on allocation depend on the relationship matrix and the specific weighting rule [7,34,35]. The more balanced holdings in this study should be understood in the context of the overall relationships among resources, manufacturing, and consumption and services, reflecting the complementary role of AI linkage information in cross-stage capital allocation.

In terms of performance, the MCoP has higher annualized returns, cumulative returns, and Sharpe ratios than both MVPs, alongside higher return volatility and a larger maximum drawdown. By comparison, the raw-return-based MVP performs better in controlling volatility and drawdowns, while the AI-Beta-based MVP lies between the other two portfolios. The MCoP's annualized return exceeds that of the raw-return-based MVP by about 2.9 percentage points, while its Sharpe ratio is higher by 0.125; annualized volatility and maximum drawdown magnitude are also higher by 1.53 and 4.64 percentage points, respectively. Its allocation implications concern both cumulative performance and the volatility and drawdowns experienced over the holding period. More balanced industrial-chain holdings thus correspond to a different return–volatility combination.

Accounting for rebalancing, the MCoP has higher turnover than the two MVPs (Table 4B). After proportional transaction costs of 5, 10, and 20 basis points per unit traded, it retains the highest cumulative return and Sharpe ratio among the three portfolios.

Table 4. Asset allocation weights, performance, and transaction-cost sensitivity. (**A**) Asset allocation weights and gross performance. (**B**) Turnover and transaction-cost-adjusted performance.

(A)

Portfolio	Matrix Source	Average Upstream Weight	Average Midstream Weight	Average Downstream Weight	Ann. Return	Ann. Volatility	Sharpe	Maximum Drawdown	Cum. Return
MCoP	AI Beta	0.34	0.35	0.31	3.89%	23.79%	0.280	−55.90%	53.82%
MVP	AI Beta	0.24	0.28	0.48	3.08%	23.43%	0.248	−54.89%	40.93%
MVP	Raw returns	0.29	0.08	0.63	0.96%	22.26%	0.155	−51.26%	11.43%

(B)

Portfolio	Matrix Source	Average Daily Turnover	5 bps	10 bps	20 bps
MCoP	AI Beta	2.14%	49.12%/0.269	44.57%/0.257	35.87%/0.234
MVP	AI Beta	1.22%	38.44%/0.241	35.99%/0.234	31.21%/0.221
MVP	Raw returns	1.70%	8.72%/0.145	6.06%/0.135	0.95%/0.116

Note: Each cost cell in (**B**) reports cumulative return (%)/Sharpe ratio. Turnover is total purchases plus sales relative to portfolio value, measured from return-adjusted pre-rebalancing weights [33].

4.3.2. Dynamic Performance

Figure 5 shows that the cumulative paths of the MCoP and MVPs share their main fluctuations while diverging during particular phases. In the early and middle parts of the sample, the MCoP lies below the two MVPs for many periods. Later in the sample, its cumulative returns rise more markedly and reach the highest level at the sample end. The MCoP's relative performance thus shifts from lagging to leading, as allocation differences associated with AI linkage information gradually emerge through the accumulation of returns across periods. The same industrial-chain assets follow different return paths under different holding structures, and the allocation role of dynamic linkage information must be assessed in conjunction with cumulative performance over the full sample.

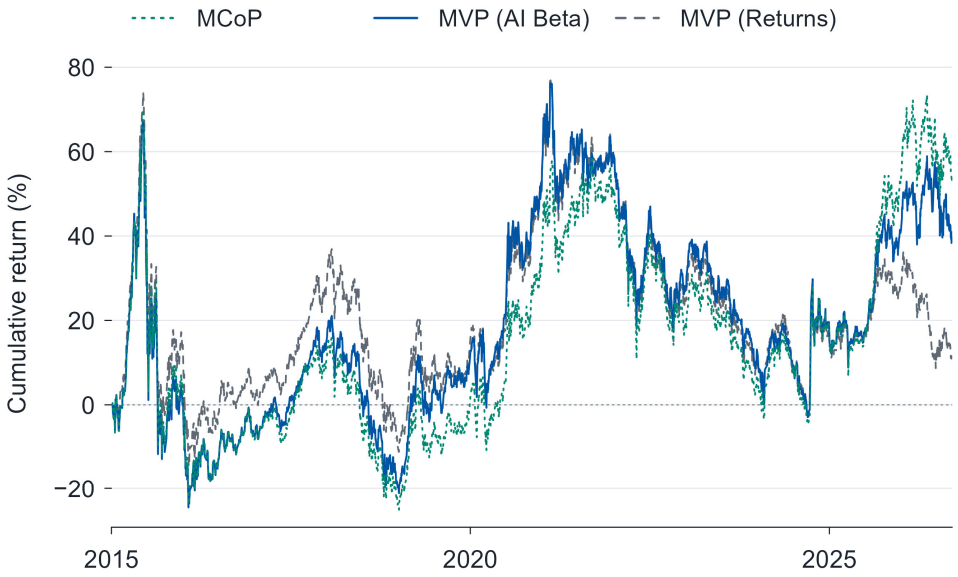


Figure 5. Cumulative returns of the MCoP and MVPs.

4.4. Robustness Tests

4.4.1. Alternative Industrial-Chain Index Series

This section replaces the CSI industrial-chain indices with the SSE Upstream Industry Index (000094), SSE Midstream Industry Index (000095), and SSE Downstream Industry Index (000096). The SSE series uses securities from the relevant industries in the Shanghai market and is constructed according to official industry classifications; historical index levels are also obtained from Wind. This substitution changes market coverage and industrial weights, while all other variable treatments and model specifications remain unchanged. Figure 6 shows broadly consistent principal fluctuations in the Betas of the two index series, supporting the similarity of sensitivity paths under alternative index constructions.

4.4.2. Alternative Conditional Distribution

To account for fat tails, this section replaces the Gaussian likelihood with a t-distribution likelihood while keeping the variable combinations, mean structures, and GARCH and DCC orders unchanged, thereby allowing a heavier-tailed innovation distribution [54]. Table 5 shows that both specifications converge and that their DCC parameter sums are below one. The residual diagnostics comprise the Q(20), Q^2(20), and ARCH-LM(10) tests of standardized marginal residuals for Y, X, and M in all models. It should be noted that the residual diagnostic tests do not reject their respective null hypotheses at the 10%

significance level. Thus, the main residual diagnostic conclusions remain unchanged under the alternative working distribution, indicating stability in the results.

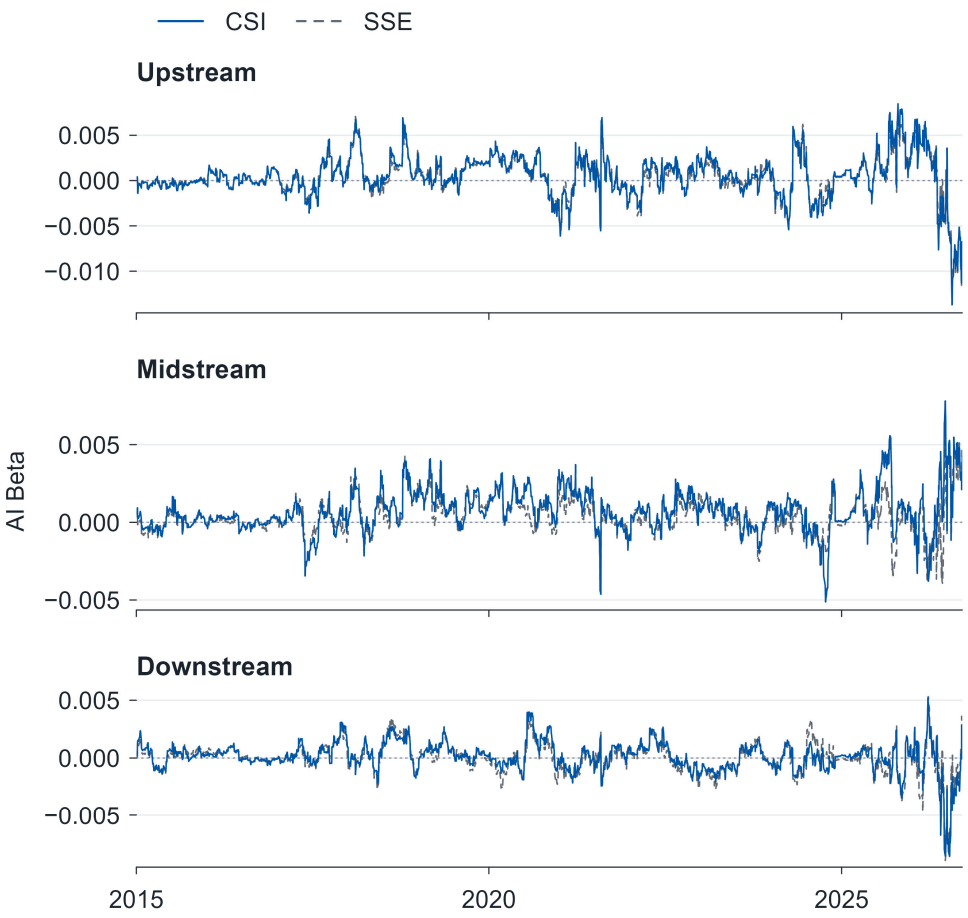


Figure 6. Comparison of dynamic Betas for the CSI and SSE industrial chains.

Table 5. DCC-ARMA-GARCH model evaluation under different conditional distributions.

Model	Residual Variable	*a*	*b*	*a* + *b*	Q(20)	$Q^2(20)$	ARCH-LM(10)	Converged
t·Upstream	Y	0.0259	0.9645	0.9905	18.268	15.893	6.722	Yes
	X				23.092	1.949	0.721	
	M				23.931	9.324	4.544	
t·Midstream	Y	0.0233	0.9642	0.9874	19.883	11.237	7.228	Yes
	X				23.092	1.949	0.721	
	M				23.931	9.324	4.544	
t·Downstream	Y	0.0285	0.9637	0.9922	22.838	13.462	7.622	Yes
	X				23.092	1.949	0.721	
	M				23.931	9.324	4.544	

Note: Y, X, and M denote the corresponding industrial-chain stage, AI, and the CSI 300, respectively. The DCC parameters *a* and *b* govern the impact of the latest standardized innovations and the carryover of the previous correlation state, respectively.

4.4.3. Alternative AI Indicator

This study further replaces the AI-E index with the AI Index, and both daily indices come from the same website. The AI Index only requires articles to contain AI-related keywords, whereas AI-E additionally requires them to contain economy-related keywords. The data analysis results remain broadly consistent. Figure 7 shows that overall linkages in both Beta systems undergo phases of strengthening and weakening and follow similar paths.

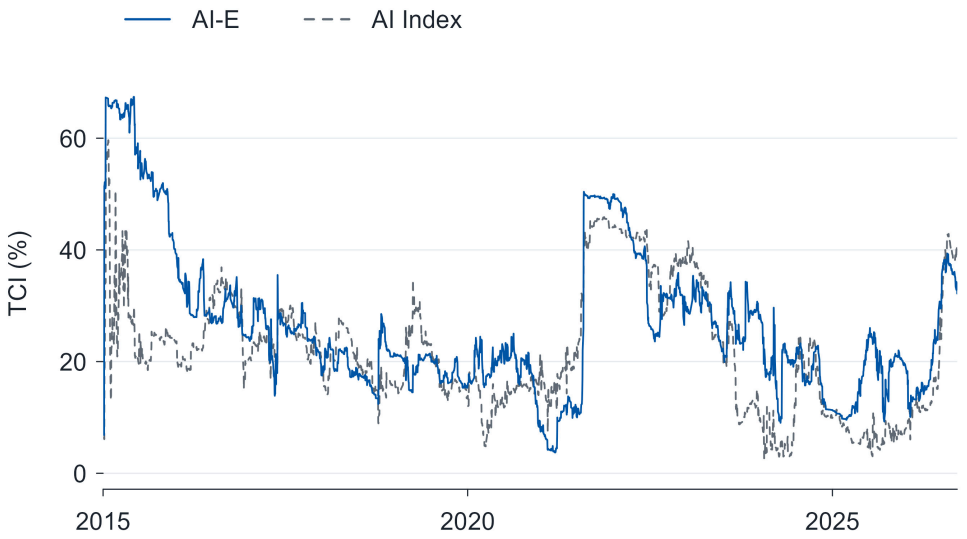


Figure 7. Comparison of dynamic TCI under the alternative AI indicator.

Table 6 shows that the MCoP continues to produce relatively diversified cross-stage allocations after the AI indicator is replaced, with a lower average midstream weight and a higher downstream weight. Under the common accounting convention, the AI-Index-driven MCoP has higher cumulative returns and a higher Sharpe ratio, together with lower volatility and a smaller maximum drawdown. Under both AI indicators, the MCoP's cumulative returns and Sharpe ratio exceed those of the corresponding MVP, reflecting allocation differences associated with linkage information and covariance information. These findings indicate that the results of this study are robust.

Table 6. Asset allocation results under the alternative AI indicator.

Portfolio	AI Indicator	Average Upstream Weight	Average Midstream Weight	Average Downstream Weight	Ann. Return	Ann. Volatility	Sharpe	Maximum Drawdown	Cum. Return
MCoP	AI-E	0.34	0.35	0.31	3.89%	23.79%	0.280	−55.90%	53.82%
MCoP	AI Index	0.34	0.31	0.35	4.50%	23.40%	0.306	−53.83%	64.39%
MVP	AI-E	0.24	0.28	0.48	3.08%	23.43%	0.248	−54.89%	40.93%
MVP	AI Index	0.18	0.29	0.53	3.55%	23.19%	0.267	−53.03%	48.35%

4.4.4. Out-of-Sample Test

This study further uses the first 70% of observations for initial estimation and conducts period-by-period portfolio evaluation over the remaining 30% using an expanding window. At each step, the model is re-estimated using observations up to the current period, and the resulting weights are applied to the next period's returns to construct the portfolios. The results remain highly consistent with the original calculations over the same evaluation period (Table 7 and Figure 8).

Table 7. Portfolio performance in the expanding-window evaluation.

Portfolio	Matrix Source	Ann. Return	Ann. Volatility	Sharpe	Maximum Drawdown	Cum. Return
MCoP	AI Beta	6.45%	19.79%	0.415	−27.52%	23.60%
MVP	AI Beta	1.72%	19.06%	0.185	−30.04%	5.96%
MVP	Raw returns	−4.48%	16.86%	−0.188	−28.43%	−14.39%

Note: The initial window contains 1993 observations. The evaluation period runs from 16 March 2023 to 18 September 2026 and contains 854 observations. The return-accounting convention is unchanged from Table 4.

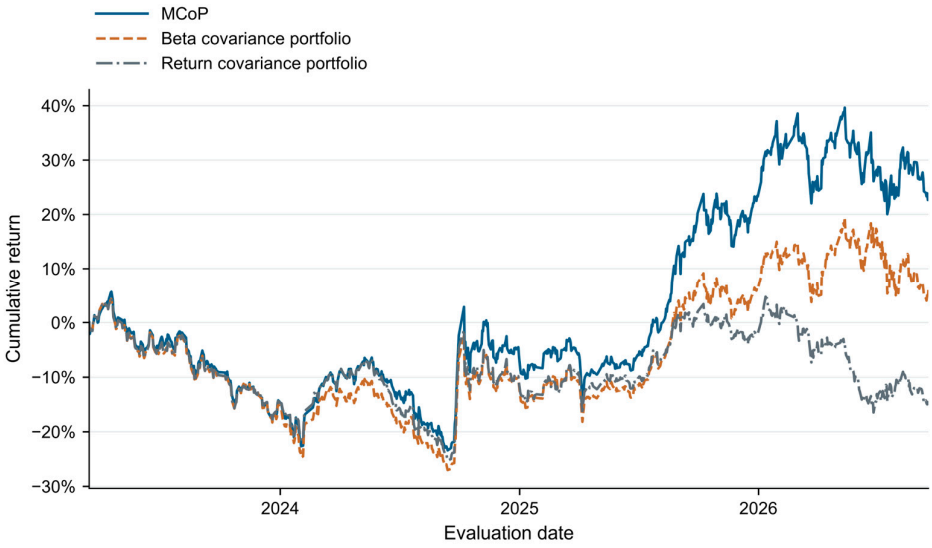


Figure 8. Cumulative returns in the expanding-window evaluation.

4.4.5. Alternative Information Factor

As a sensitivity analysis, we replace AI-E with the Economic Uncertainty index while keeping the sample and model settings unchanged. The two TCI paths display clear differences (Figure 9), indicating that the estimated connectedness dynamics vary with the information factor considered.

4.4.6. Alternative Forecast Horizons

In addition, we examine the sensitivity of the connectedness results to the forecast horizon by comparing variance decompositions over 10, 20, and 50 periods. Figure 10 shows broadly consistent temporal fluctuations in the TCI across these horizons, supporting the robustness of the identified pattern of dynamic connectedness.

4.4.7. Alternative Forgetting Factors

Figure 11 presents the dynamic TCI under forgetting factors of 0.99, 0.985, and 0.975. The three specifications exhibit broadly consistent temporal patterns, supporting robustness.

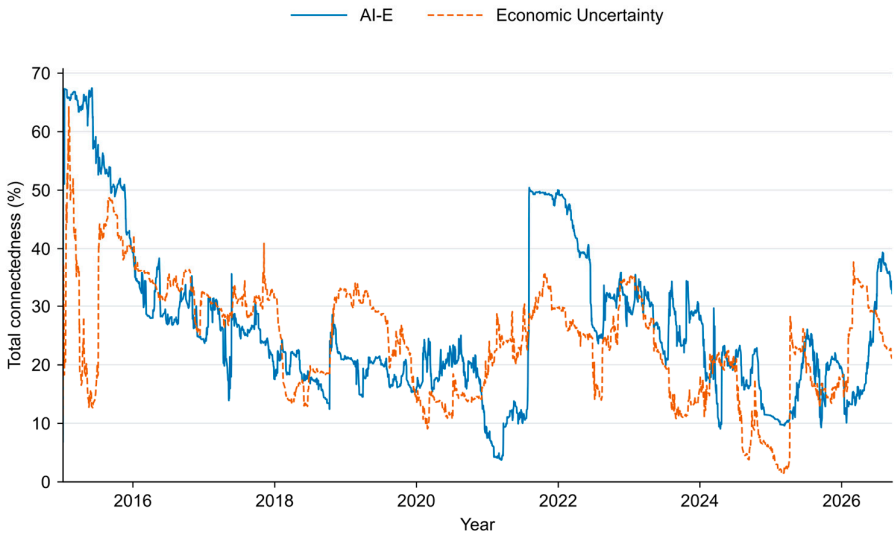


Figure 9. TCI comparison between AI-E and Economic Uncertainty.

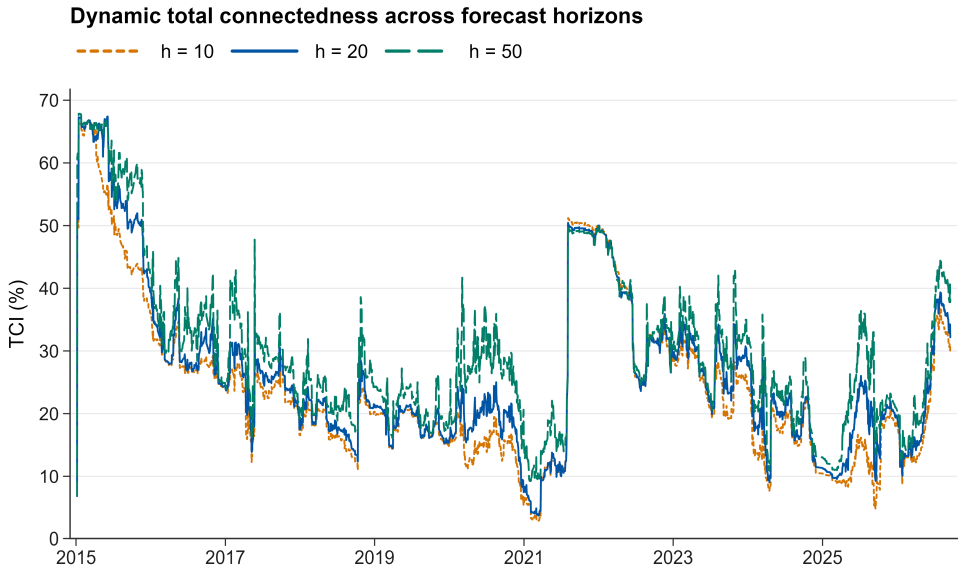


Figure 10. Dynamic TCI at different forecast horizons.

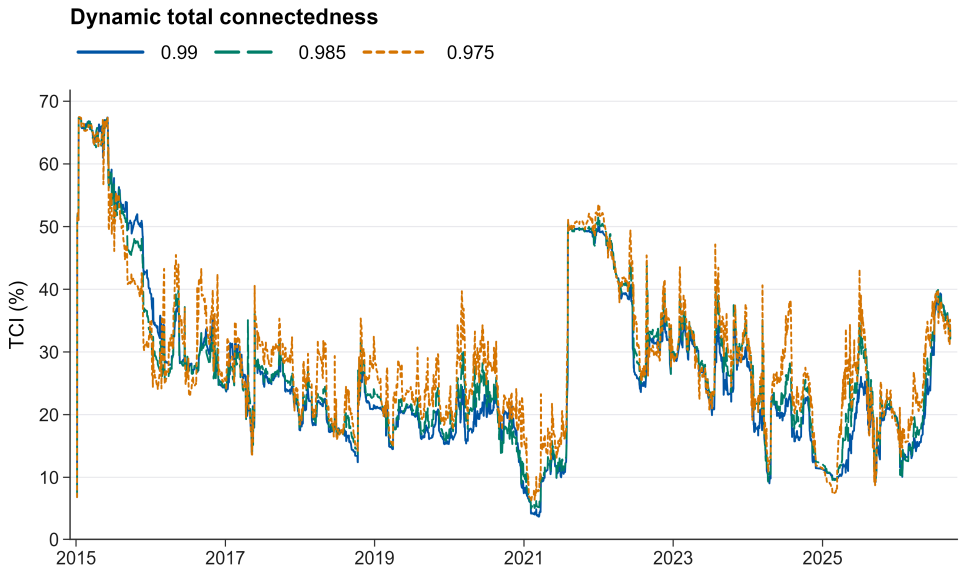


Figure 11. Dynamic TCI under alternative coefficient-state forgetting factors.

5. Conclusions and Implications

This study examines dynamic linkages and asset allocation across China's industrial chain in the AI era, distinguishing overall industrial-chain linkages from cross-stage AI sensitivity linkages. It extracts dynamic AI Betas for the upstream, midstream, and downstream stages using trivariate DCC-ARMA-GARCH models, employs TVP-VAR to characterize their linkage strength, net transmission structure, and phase-specific changes, and uses AI sensitivity linkage information to construct allocation weights. The analysis thereby extends the perspective from each stage's individual response to AI changes to the interrelationships among sensitivity adjustments, and further examines the holding structures and allocation performance associated with this relational information.

Three main conclusions emerge. First, AI sensitivities along the industrial chain combine own-stage dynamics with cross-stage relationships, whereas raw returns exhibit stronger overall linkages. This indicates that common price movements and AI sensitivity adjustments have different association structures, with the AI perspective further revealing stage-level differences within overall market comovement. Second, the static AI Beta network features the upstream stage as the principal net transmitter and the midstream stage as the principal net receiver, while the raw return network features the midstream stage as the principal net transmitter. The dynamic results further show that node roles in the AI sensitivity network are more distinctly phase-dependent. The same industrial stage assumes different transmission roles across information dimensions, making industrial-chain financial relationships information-dependent and time-varying. Third, compared with the MVPs constructed from AI Beta covariances and raw return covariances, the MCoP driven by the AI Beta linkage structure produces more balanced average cross-stage allocations and higher cumulative returns. This finding extends the relevance of AI sensitivity linkage analysis to asset allocation, indicating that relational information across stages can complement covariance-oriented industrial-chain allocation.

Accordingly, this study offers the following implications for industrial policy evaluation and investment management. First, account for stage-specific differences and cross-stage linkages when evaluating AI industrial policies. Given that upstream, midstream, and downstream AI sensitivities have both distinctive characteristics and interrelationships, AI-related market responses can be used as supplementary information for

observing industrial-chain changes, taking into account the technological foundations and operating characteristics of each stage. Combining this information with actual firm-level AI applications and needs can inform policy evaluations for the resources, manufacturing, and consumption and services stages. This is consistent with the sector-specific implementation and intelligent supply-chain coordination emphasized by the "AI Plus" policy.

Second, distinguish information sources in dynamic industrial-chain monitoring. Incorporate overall return linkages and AI sensitivity linkages into a complementary monitoring framework to track cross-stage linkage strength, principal transmission nodes, and changes in their roles. Assess financial market signals alongside information on business operations, input–output relationships, and technology applications, and adjust monitoring priorities according to linkage structures in different periods to inform industrial administration and financial regulatory authorities about industrial-chain dynamics.

Third, use relational information as a supplementary basis for industrial-chain asset allocation. Institutional investors can compare different holding structures using cross-stage AI sensitivity linkages alongside covariance analysis and comprehensively assess returns, volatility, and drawdowns. Practical implementation of the strategy can further incorporate transaction costs, holding constraints, and out-of-sample tests to examine the persistence of allocation performance. The findings can also serve as a reference for research on index instruments for cross-industry allocation and are relevant to the policy direction of strengthening the asset allocation function of index funds.

The measurement scope of this study is confined to AI-related economic information captured by newspaper coverage. Future research could incorporate firm-level data on AI adoption, investment expenditure, and utilization intensity to examine how information-related market responses connect with actual AI implementation across industrial-chain stages. This study uses three broad Chinese industrial-chain indices representing the upstream, midstream, and downstream stages. Future research could examine more detailed industry classifications and extend the analysis to other countries, markets, and periods.

Author Contributions: Conceptualization, X.Y. and W.G.; methodology, X.Y. and W.G.; software, W.G.; validation, X.Y., W.G. and Y.J.; formal analysis, X.Y. and W.G.; investigation, X.Y. and W.G.; data curation, X.Y. and W.G.; writing—original draft preparation, X.Y. and W.G.; writing—review and editing, X.Y., W.G. and Y.J.; visualization, W.G.; supervision, Y.J. All authors have read and agreed to the published version of the manuscript.

Funding: This research was supported by Hebei Natural Science Foundation (G2026207018).

Data Availability Statement: The original contributions presented in this study are included in the article. Further inquiries can be directed to the corresponding author.

Conflicts of Interest: The authors declare no conflicts of interest.

References

1. Bresnahan, T.F.; Trajtenberg, M. General purpose technologies 'Engines of growth'? *J. Econom.* **1995**, *65*, 83–108. https://doi.org/10.1016/0304-4076(94)01598-T.
2. Brynjolfsson, E.; Rock, D.; Syverson, C. The Productivity J-Curve: How Intangibles Complement General Purpose Technologies. *Am. Econ. J. Macroecon.* **2021**, *13*, 333–372. https://doi.org/10.1257/mac.20180386.
3. Noy, S.; Zhang, W. Experimental evidence on the productivity effects of generative artificial intelligence. *Science* **2023**, *381*, 187–192. https://doi.org/10.1126/science.adh2586.
4. Brynjolfsson, E.; Li, D.; Raymond, L. Generative AI at Work. *Q. J. Econ.* **2025**, *140*, 889–942. https://doi.org/10.1093/qje/qjae044.
5. Carvalho, V.M.; Tahbaz-Salehi, A. Production Networks: A Primer. *Annu. Rev. Econ.* **2019**, *11*, 635–663. https://doi.org/10.1146/annurev-economics-080218-030212.
6. Cohen, L.; Frazzini, A. Economic Links and Predictable Returns. *J. Financ.* **2008**, *63*, 1977–2011. https://doi.org/10.1111/j.1540-6261.2008.01379.x.

7. Broadstock, D.C.; Chatziantoniou, I.; Gabauer, D. Minimum Connectedness Portfolios and the Market for Green Bonds: Advocating Socially Responsible Investment (SRI) Activity. In *Applications in Energy Finance: The Energy Sector, Economic Activity, Financial Markets and the Environment*; Floros, C., Chatziantoniou, I., Eds.; Palgrave Macmillan: Cham, Switzerland, 2022; pp. 217–253. https://doi.org/10.1007/978-3-030-92957-2_9.
8. Felten, E.; Raj, M.; Seamans, R. Occupational, industry, and geographic exposure to artificial intelligence: A novel dataset and its potential uses. *Strateg. Manag. J.* **2021**, *42*, 2195–2217. https://doi.org/10.1002/smj.3286.
9. Babina, T.; Fedyk, A.; He, A.; Hodson, J. Artificial Intelligence, Firm Growth, and Product Innovation. *J. Financ. Econ.* **2024**, *151*, 103745. https://doi.org/10.1016/j.jfineco.2023.103745.
10. Acemoglu, D.; Carvalho, V.M.; Ozdaglar, A.; Tahbaz-Salehi, A. The Network Origins of Aggregate Fluctuations. *Econometrica* **2012**, *80*, 1977–2016. https://doi.org/10.3982/ECTA9623.
11. Carvalho, V.M. From Micro to Macro via Production Networks. *J. Econ. Perspect.* **2014**, *28*, 23–48. https://doi.org/10.1257/jep.28.4.23.
12. Baqaee, D.R.; Farhi, E. The Macroeconomic Impact of Microeconomic Shocks: Beyond Hulten's Theorem. *Econometrica* **2019**, *87*, 1155–1203. https://doi.org/10.3982/ECTA15202.
13. Acemoglu, D.; Azar, P.D. Endogenous Production Networks. *Econometrica* **2020**, *88*, 33–82. https://doi.org/10.3982/ECTA15899.
14. Barrot, J.-N.; Sauvagnat, J. Input Specificity and the Propagation of Idiosyncratic Shocks in Production Networks. *Q. J. Econ.* **2016**, *131*, 1543–1592. https://doi.org/10.1093/qje/qjw018.
15. Carvalho, V.M.; Nirei, M.; Saito, Y.U.; Tahbaz-Salehi, A. Supply Chain Disruptions: Evidence from the Great East Japan Earthquake. *Q. J. Econ.* **2021**, *136*, 1255–1321. https://doi.org/10.1093/qje/qjaa044.
16. Herskovic, B. Networks in Production: Asset Pricing Implications. *J. Financ.* **2018**, *73*, 1785–1818. https://doi.org/10.1111/jofi.12684.
17. Gofman, M.; Segal, G.; Wu, Y. Production Networks and Stock Returns: The Role of Vertical Creative Destruction. *Rev. Financ. Stud.* **2020**, *33*, 5856–5905. https://doi.org/10.1093/rfs/hhaa034.
18. Hou, K. Industry Information Diffusion and the Lead-Lag Effect in Stock Returns. *Rev. Financ. Stud.* **2007**, *20*, 1113–1138. https://doi.org/10.1093/revfin/hhm003.
19. Menzly, L.; Ozbas, O. Market Segmentation and Cross-predictability of Returns. *J. Financ.* **2010**, *65*, 1555–1580. https://doi.org/10.1111/j.1540-6261.2010.01578.x.
20. Hong, H.; Torous, W.; Valkanov, R. Do industries lead stock markets? *J. Financ. Econ.* **2007**, *83*, 367–396. https://doi.org/10.1016/j.jfineco.2005.09.010.
21. Cen, L.; Hertzel, M.; Schiller, C. Speed Matters: Limited Attention and Supply Chain Information Diffusion. *Manag. Sci.* **2025**, *71*, 8642–8669. https://doi.org/10.1287/mnsc.2023.00291.
22. Lee, C.M.C.; Sun, S.T.; Wang, R.; Zhang, R. Technological links and predictable returns. *J. Financ. Econ.* **2019**, *132*, 76–96. https://doi.org/10.1016/j.jfineco.2018.11.008.
23. Goldfarb, A.; Taska, B.; Teodoridis, F. Could machine learning be a general purpose technology? A comparison of emerging technologies using data from online job postings. *Res. Policy* **2023**, *52*, 104653. https://doi.org/10.1016/j.respol.2022.104653.
24. McElheran, K.; Li, J.F.; Brynjolfsson, E.; Kroff, Z.; Dinlersoz, E.; Foster, L.; Zolas, N. AI adoption in America: Who, what, and where. *J. Econ. Manag. Strategy* **2024**, *33*, 375–415. https://doi.org/10.1111/jems.12576.
25. Raisch, S.; Krakowski, S. Artificial Intelligence and Management: The Automation–Augmentation Paradox. *Acad. Manag. Rev.* **2021**, *46*, 192–210. https://doi.org/10.5465/amr.2018.0072.
26. Agrawal, A.; Gans, J.S.; Goldfarb, A. Artificial intelligence adoption and system-wide change. *J. Econ. Manag. Strategy* **2024**, *33*, 327–337. https://doi.org/10.1111/jems.12521.
27. Acemoglu, D.; Autor, D.; Hazell, J.; Restrepo, P. Artificial Intelligence and Jobs: Evidence from Online Vacancies. *J. Labor Econ.* **2022**, *40*, S293–S340. https://doi.org/10.1086/718327.
28. Beraja, M.; Yang, D.Y.; Yuchtman, N. Data-intensive Innovation and the State: Evidence from AI Firms in China. *Rev. Econ. Stud.* **2023**, *90*, 1701–1723. https://doi.org/10.1093/restud/rdac056.
29. Eisfeldt, A.L.; Schubert, G. Generative AI and Finance. *Annu. Rev. Financ. Econ.* **2025**, *17*, 363–393. https://doi.org/10.1146/annurev-financial-112923-020503.
30. Acemoglu, D. The simple macroeconomics of AI. *Econ. Policy* **2025**, *40*, 13–58. https://doi.org/10.1093/epolic/eiae042.
31. Markowitz, H. Portfolio Selection. *J. Financ.* **1952**, *7*, 77–91. https://doi.org/10.1111/j.1540-6261.1952.tb01525.x.
32. Buraschi, A.; Porchia, P.; Trojani, F. Correlation Risk and Optimal Portfolio Choice. *J. Financ.* **2010**, *65*, 393–420. https://doi.org/10.1111/j.1540-6261.2009.01533.x.

33. DeMiguel, V.; Garlappi, L.; Uppal, R. Optimal Versus Naive Diversification: How Inefficient is the 1/N Portfolio Strategy? *Rev. Financ. Stud.* **2009**, *22*, 1915–1953. https://doi.org/10.1093/rfs/hhm075.
34. Peralta, G.; Zareei, A. A Network Approach to Portfolio Selection. *J. Empir. Financ.* **2016**, *38*, 157–180. https://doi.org/10.1016/j.jempfin.2016.06.003.
35. Výrost, T.; Lyócsa, Š.; Baumöhl, E. Network-Based Asset Allocation Strategies. *N. Am. J. Econ. Financ.* **2019**, *47*, 516–536. https://doi.org/10.1016/j.najef.2018.06.008.
36. Fama, E.F.; French, K.R. Common Risk Factors in the Returns on Stocks and Bonds. *J. Financ. Econ.* **1993**, *33*, 3–56. https://doi.org/10.1016/0304-405X(93)90023-5.
37. Engle, R.F. Dynamic Conditional Beta. *J. Financ. Econom.* **2016**, *14*, 643–667. https://doi.org/10.1093/jjfinec/nbw006.
38. Du, J.; Cao, W.; Wang, Z. Forecasting Risk Matrices with Economic Policy Uncertainty and Financial Stress: A Machine Learning Approach. *Mathematics* **2026**, *14*, 938. https://doi.org/10.3390/math14060938.
39. Bollerslev, T. Generalized Autoregressive Conditional Heteroskedasticity. *J. Econom.* **1986**, *31*, 307–327. https://doi.org/10.1016/0304-4076(86)90063-1.
40. Engle, R.F. Dynamic Conditional Correlation: A Simple Class of Multivariate Generalized Autoregressive Conditional Heteroskedasticity Models. *J. Bus. Econ. Stat.* **2002**, *20*, 339–350. https://doi.org/10.1198/073500102288618487.
41. Antonakakis, N.; Chatziantoniou, I.; Gabauer, D. Refined Measures of Dynamic Connectedness Based on Time-Varying Parameter Vector Autoregressions. *J. Risk Financ. Manag.* **2020**, *13*, 84. https://doi.org/10.3390/jrfm13040084.
42. Schwarz, G. Estimating the Dimension of a Model. *Ann. Stat.* **1978**, *6*, 461–464. https://doi.org/10.1214/aos/1176344136.
43. Koop, G.; Korobilis, D. Large Time-Varying Parameter VARs. *J. Econom.* **2013**, *177*, 185–198. https://doi.org/10.1016/j.jeconom.2013.04.007.
44. Pesaran, M.H.; Shin, Y. Generalized Impulse Response Analysis in Linear Multivariate Models. *Econ. Lett.* **1998**, *58*, 17–29. https://doi.org/10.1016/S0165-1765(97)00214-0.
45. Diebold, F.X.; Yilmaz, K. Better to Give Than to Receive: Predictive Directional Measurement of Volatility Spillovers. *Int. J. Forecast.* **2012**, *28*, 57–66. https://doi.org/10.1016/j.ijforecast.2011.02.006.
46. Diebold, F.X.; Yilmaz, K. On the Network Topology of Variance Decompositions: Measuring the Connectedness of Financial Firms. *J. Econom.* **2014**, *182*, 119–134. https://doi.org/10.1016/j.jeconom.2014.04.012.
47. Gaies, B. AI Uncertainty and Global Stock Market Volatility: Any Signals of a Dot-com 2.0? *Econ. Lett.* **2026**, *264*, 112954. https://doi.org/10.1016/j.econlet.2026.112954.
48. Yilmazkuday, H. ChatGPT and Stock Returns. *J. Econ. Finance* **2026**, *50*, 29. https://doi.org/10.1007/s12197-026-09767-9.
49. Jarque, C.M.; Bera, A.K. A Test for Normality of Observations and Regression Residuals. *Int. Stat. Rev.* **1987**, *55*, 163–172. https://doi.org/10.2307/1403192.
50. Dickey, D.A.; Fuller, W.A. Distribution of the Estimators for Autoregressive Time Series with a Unit Root. *J. Am. Stat. Assoc.* **1979**, *74*, 427–431. https://doi.org/10.1080/01621459.1979.10482531.
51. Phillips, P.C.B.; Perron, P. Testing for a Unit Root in Time Series Regression. *Biometrika* **1988**, *75*, 335–346. https://doi.org/10.1093/biomet/75.2.335.
52. Ljung, G.M.; Box, G.E.P. On a Measure of Lack of Fit in Time Series Models. *Biometrika* **1978**, *65*, 297–303. https://doi.org/10.1093/biomet/65.2.297.
53. Engle, R.F. Autoregressive Conditional Heteroscedasticity with Estimates of the Variance of United Kingdom Inflation. *Econometrica* **1982**, *50*, 987–1007. https://doi.org/10.2307/1912773.
54. Bollerslev, T. A Conditionally Heteroskedastic Time Series Model for Speculative Prices and Rates of Return. *Rev. Econ. Stat.* **1987**, *69*, 542–547. https://doi.org/10.2307/1925546.

Disclaimer/Publisher's Note: The statements, opinions and data contained in all publications are solely those of the individual author(s) and contributor(s) and not of MDPI and/or the editor(s). MDPI and/or the editor(s) disclaim responsibility for any injury to people or property resulting from any ideas, methods, instructions or products referred to in the content.